

# Resonant amplification of the Andreev process in ballistic Josephson junctions

Ivana Petković<sup>1,2</sup>, Nikolai M. Chtchelkatchev<sup>3,4</sup>, and Zoran Radović<sup>1</sup>

<sup>1</sup> *Department of Physics, University of Belgrade, P.O. Box 368, 11001 Belgrade, Serbia and Montenegro*

<sup>2</sup> *Laboratoire de Physique des Solides, Batiment 510, 91405 Orsay, France*

<sup>3</sup> *L.D. Landau Institute for Theoretical Physics, RAS, 117940 Moscow, Russia*

<sup>4</sup> *Institute for High Pressure Physics, RAS, 142092 Troitsk, Russia*

We study the Josephson effect in ballistic SINIS and SIFIS double-barrier junctions, consisting of superconductors (S), a clean normal (N) or ferromagnetic (F) metal, and insulating interfaces (I). For short SINIS double-tunnel junctions with one channel open for quasiparticle propagation, the critical Josephson current as a function of the junction width shows sharp peaks because of a resonant amplification of the Andreev process: when the quasibound states of the normal interlayer enter the superconducting gap the Andreev bound states are lowered down to the Fermi level. For corresponding SIFIS junctions the quasibound states are spin-split; they amplify the supercurrent less efficiently, and trigger transitions between 0 and  $\pi$  states of the junction. In contrast to SINIS junctions, a narrow dip related to the  $0 - \pi$  transition opens up exactly at the peak due to a compensation of partial currents flowing in opposite directions. With an increased barrier transparency these features are gradually lost, due to the broadening and overlap of quasibound states. Temperature-induced transitions both from 0 to  $\pi$  and from  $\pi$  to 0 states are studied by computing the phase diagram (with temperature and junction width as the variables) for different interfacial transparencies varying from metallic to the tunnel limit.

PACS numbers: 74.50.+r, 74.45.+c

## I. INTRODUCTION

Recently, many interesting phenomena were investigated in superconductor (S) - ferromagnet (F) Josephson junctions.<sup>1,2</sup> One of the most interesting effects is the so-called  $\pi$  state of SFS junctions, in which the ground state is characterized by an intrinsic phase difference  $\phi = \pi$  between two superconductors.<sup>3,4,5,6,7,8,9,10</sup> The  $\pi$  junctions could also have important applications, such as for quantum qubits.<sup>11</sup> The Josephson effect in double-barrier SIFIS junctions, with a clean metallic ferromagnet between two insulating interfaces (I), has been studied by solving the scattering problem based on the Bogoliubov - de Gennes equation; it was found that spin-split quasiparticle transmission resonances contribute significantly to the Andreev process.<sup>12,13</sup> A comprehensive numerical study of clean layered S/F heterostructures has also been given recently.<sup>14</sup>

For SINIS structures (with a clean non ferromagnetic normal metal N), sharp peaks occur in the critical Josephson current  $I_C$  as a function of the junction width  $d$  for each transverse channel. This is the result of a resonant amplification of the Andreev process when the quasibound states in the INI interlayer approach the Fermi level. This effect is the superconducting analog of the Bohm resonant tunneling,<sup>15</sup> previously studied in Refs.<sup>16,17,18,19</sup> For corresponding SIFIS junctions, the resonant nature of  $0 - \pi$  transitions comes into play in the tunnel limit. Triggering of the  $0 - \pi$  transitions by resonant amplification, as well as the coexistence of stable and metastable 0 and  $\pi$  states in the vicinity of the transition,<sup>20,21</sup> can be fully understood. In contrast to SINIS junctions where the critical current reaches a peak value when the Andreev bound states cross the Fermi

level, here a narrow dip related to the  $0 - \pi$  transition opens up exactly at the peak due to the compensation of partial currents flowing in opposite directions. We emphasize that this is not the case for a higher interface transparency due to the broadening and overlap of quasibound states, nor for planar junctions.<sup>12</sup> Experimentally, SIFIS nanostructures could be realized, for example, in gated heterostructures,<sup>22</sup> ferromagnetic nanoparticles,<sup>23</sup> or in the break junctions<sup>24</sup> in external magnetic field producing the Zeeman splitting of Andreev levels.<sup>25</sup>

It has become a paradigm that in the  $\pi$  state of SFIS junctions, with a thin barrier of insulating ferromagnet (Fi), there is net spin polarization of current-carrying Andreev levels.<sup>26,27,28</sup> However this “rule” is not quite general. In this paper we show that in low-transparent SIFIS nanostructures with one open transverse channel the situation can be the opposite. We can generalize the previous rule: the  $0 - \pi$  transition is accompanied by the switching of the net spin polarization of current-carrying Andreev levels. The critical current oscillates as a function of the junction width, and the resonant amplification occurs when quasibound states of the ferromagnet between two insulating layers enter the gap. The  $0 - \pi$  transitions take place when Andreev levels intersect at the Fermi energy, being accompanied by a switching of their spin polarization. Experiments show that the  $\pi$  state of a dirty SFS junction can correspond to lower temperatures than the 0 state.<sup>6</sup> The theory of ballistic one-barrier SFS junctions predicts the opposite.<sup>27,29</sup> We demonstrate that in the phase diagram of double-barrier ballistic SIFIS junctions the  $\pi$  state can correspond to lower temperatures than the 0 state, depending on parameters.

## II. JOSEPHSON CURRENT

We consider a ballistic double-barrier Josephson junction: a normal-metal (N) or ferromagnetic (F) interlayer of thickness  $d$  is connected to superconductors (S) by insulating non-magnetic interfaces ( $I_1$ ,  $I_2$ ), see Fig. 1. We assume that both metals are clean and that the left and the right superconductors are equal with the constant pair potential  $\Delta \exp(\pm i\phi/2)$ , where  $\phi$  is the macroscopic phase difference across the junction. Within the Stoner model, the ferromagnet is characterized by the exchange potential  $h$ , and the insulating interfaces are modeled by  $\delta$ -function potential barriers.<sup>12,27</sup>

The Josephson current can be expressed in terms of the free energy of the junction as

$$I(\phi) = -\frac{2e}{\hbar} \partial_\phi F(\phi), \quad (1)$$

where the phase-dependent part of the junction free energy,  $F(\phi)$ , is given by

$$F(\phi) = -k_B T \sum_{n\sigma} \ln \left[ 2 \cosh \left( \frac{E_{n\sigma}(\phi)}{2k_B T} \right) \right]. \quad (2)$$

Here,  $E_{n\sigma}(\phi)$  are the Andreev levels measured with respect to the chemical potential,  $n$  denotes a transverse channel, and  $\sigma = \pm 1$  is the spin quantum number.

Assuming the SIFIS junction shorter than the superconducting coherence length, we can calculate the Josephson current using the relation

$$I(\phi) = \frac{2e}{\hbar} \sum_{n\sigma} f_{n\sigma}(T) \partial_\phi E_{n\sigma}(\phi), \quad (3)$$

where  $f_{n\sigma}(T)$  is the Fermi distribution, and  $E_{n\sigma}(\phi)$  are zeroes of the common denominator of the scattering amplitudes  $G$ , calculated from the Bogoliubov - de Gennes equation and given by Eq. (17) in Ref.<sup>12</sup>

In the following, we assume that only one channel ( $n = 1$ ) is open in the short superconducting junction. Without a ferromagnetic region there are two spin degenerate Andreev levels with the same absolute value of energy, but with the opposite sign that can be parametrized by  $\eta = \pm 1$ . The ferromagnet spin-splits Andreev levels, and there are four of them,  $E_{\eta\sigma}(\phi)$ . We will express  $E_{\eta\sigma}(\phi)$  explicitly in terms of the scattering matrix.<sup>27,29</sup> For the IFI structure formed by the ferromagnet and two insulating barriers we define  $t_\pm$  and  $r_\pm$  to be the absolute values of the electron and hole transmission and reflection amplitudes,  $\hat{t}(\pm E, \sigma)$  and  $\hat{r}(\pm E, \sigma)$ , where  $E$  is the quasiparticle energy with respect to the chemical potential. The corresponding phases are denoted as  $\chi_\pm^t$  and  $\chi_\pm^r$ . The Andreev levels can be calculated as roots of the equation

$$\cos(\Phi - 2\alpha) - \cos \gamma = 0, \quad (4)$$

where  $\gamma$  is defined by

$$\cos \gamma = r_+ r_- \cos \beta + t_+ t_- \cos \phi. \quad (5)$$

Here,  $\alpha = \arccos(E/\Delta)$ ,  $\Phi = \chi_+^t - \chi_-^t$ , and  $\beta = (\chi_+^t - \chi_+^r) - (\chi_-^t - \chi_-^r)$ . From Eq. (4) the Andreev levels are

$$E_{\eta\sigma}(\phi) = \Delta \cos \left( \frac{\Phi_0 + \eta\gamma_0}{2} \right) \text{sign} \left[ \sin \left( \frac{\Phi_0 + \eta\gamma_0}{2} \right) \right], \quad (6)$$

where  $\Phi_0 = \Phi(E = 0, \sigma)$  and  $\gamma_0 = \gamma(E = 0, \sigma)$ . In the limiting case of a single insulating barrier this formula reduces to the corresponding equations found in Refs. [27,28,29]. Using Eq. (5) in the form  $\partial_\phi \gamma = t_+ t_- \sin \phi / \sin \gamma$ , we finally obtain

$$I(\phi) = \sum_{\sigma, \eta = \pm 1} \frac{e\Delta}{2\hbar} \frac{t_+ t_- \sin \phi}{\sin \gamma_0} \sin \left( \frac{\gamma_0 + \eta\Phi_0}{2} \right) \tanh \frac{E_{\eta\sigma}(\phi)}{2k_B T}, \quad (7)$$

which is a generalization of Eq. (3) in Ref. [27]. The transmission amplitudes of the IFI structure can be expressed through the transmission and reflection amplitudes of the insulating barriers,  $\hat{t}_{I_{1,2}}$ ,  $\hat{r}_{I_{1,2}}$ , and the momentum of an electron in F,  $q_\sigma(E) = \sqrt{2m(E_F^{(F)} + E + \sigma h)}$ , and in S,  $k = \sqrt{2m(E_F^{(S)} + \Omega)}$ , where  $\Omega = \sqrt{E^2 - \Delta^2}$ . Namely,

$$\begin{aligned} \hat{t}(E, \sigma) &= \frac{\hat{t}_{I_1} \hat{t}_{I_2} e^{i(q_\sigma - k)d}}{1 - \hat{r}'_{I_1} \hat{r}_{I_2} e^{2iq_\sigma d}}, \\ \hat{r}(E, \sigma) &= r_{I_1} e^{-ikd} + \frac{(\hat{t}_{I_1} e^{i(q_\sigma - k)d/2})^2 r_{I_2} e^{iq_\sigma d}}{1 - \hat{r}'_{I_1} \hat{r}_{I_2} e^{2iq_\sigma d}}. \end{aligned} \quad (8)$$

Note that the expression for the transmission amplitude has the same form as the one for the Fabry-Perot interferometer. Here, the scattering amplitudes of the insulating barriers are

$$\begin{aligned} \hat{t}_{I_{1,2}} &= \frac{2\sqrt{kq_\sigma}}{k + q_\sigma + 2iZ_{1,2}k_F^{(S)}}, \\ \hat{r}_{I_{1,2}} &= \frac{k - q_\sigma - 2iZ_{1,2}k_F^{(S)}}{k + q_\sigma + 2iZ_{1,2}k_F^{(S)}}, \end{aligned} \quad (9)$$

where  $k_F^{(S)} = \sqrt{2mE_F^{(S)}}$ , the parameters  $Z_{1,2}$  determine transmission probabilities of insulating barriers, and  $r' = -r^*/t^*$  (\* denotes the complex conjugation). In the tunnel limit,  $|\hat{t}_{I_{1,2}}| \rightarrow 0$ , the positions of the bound states are simply given by the conditions  $dq_\sigma(+E) = n_1\pi$  and  $dq_\sigma(-E) = n_2\pi$ , where  $n_1$  and  $n_2$  are integers.

The results are illustrated in Figs. 2–11. In all illustrations superconductors are characterized by  $\Delta/E_F^{(S)} = 10^{-3}$ , the Fermi energies of the two metals are equal,  $E_F^{(F)} = E_F^{(S)}$ , in F or N interlayers the normalized exchange energy is  $X = h/E_F^{(F)} = 0.1$  or 0, and the

insulating barriers are assumed to be equal and characterized by the common parameter  $Z_1 = Z_2 = Z$ , related to the one-barrier transmission probability via  $|\hat{t}_{I_1}|^2 = |\hat{t}_{I_2}|^2 = 1/(1 + Z^2)$ .

In SINIS double-tunnel junctions sharp peaks occur in the critical Josephson current as the junction width is varied (Fig. 2, top panel) because of resonant amplification of the Andreev process when the quasibound states of the INI interlayer enter the superconducting gap and lower the phase-sensitive Andreev bound states down to the Fermi level (Fig. 3). The order of magnitude of the peaks is the same as the critical Josephson current values in transparent junctions. Between two peaks, the junction behaves as a usual SIS junction. In this case, quasibound states are not in the superconducting gap.

In SIFIS junctions the critical current significantly decreases if the junction transparency is reduced (Fig. 2, bottom panel). Instead of the critical current reaching a peak value, in the case of low transparency a narrow dip opens up exactly at the peak due to the onset of the  $0 - \pi$  transition. Note that the modulation of spike heights in  $I_C(d)$  is due to the modulation of the Zeeman splitting. When the Zeeman-split quasibound states are closer, the amplification is larger, the peaks tend to the SNS value, and there is no triggering of the  $0 - \pi$  transition. Therefore, only the large enough spin splitting of sharp enough quasibound states can trigger the  $0 - \pi$  transition. At the transitions, spin-unpolarized Andreev states (with opposite spin orientation on the same side of the Fermi surface) become spin polarized, and vice versa. This is shown for two neighboring peaks in Fig. 4. We point out that, in contrast to the one-barrier problem,<sup>27,28,29</sup> or transparent interfaces, neither spin-polarized Andreev states have to correspond to the  $\pi$  state of the junction, nor spin-unpolarized to the  $0$  state. The following generalization is valid: every  $0 - \pi$  transition is accompanied by a switching of the spin polarization of Andreev bound states, Fig. 5. For low transparency, switching of the spin polarization is not always accompanied by  $0 - \pi$  transitions. Partial contributions of Andreev states to  $I(\phi)$  are shown in Fig. 6. In the transition region, there is a coexistence of stable and metastable  $0$  and  $\pi$  states due to a considerable contribution of the second harmonic in  $I(\phi)$ , Fig. 6.<sup>20</sup> In the tunnel limit,  $Z \rightarrow \infty$ , the Andreev bound states that are practically  $\phi$  independent coincide with bound states of the corresponding isolated normal-metal interlayer, but with nonmatching spin polarization. Because of this, the critical current is extremely weak.

With increased barrier transparency, the mechanism of  $0 - \pi$  transitions, described above, is modified by a broadening and overlap of quasibound states in the normal interlayer. In the case of complete transparency, the critical current modulation is related to only two transitions in the considered interval of  $dk_F$ , Fig. 2, bottom panel. This modulation is due to a finite width of quasibound states even for transparent interfaces because of the mismatch of Fermi energies for different spins resulting in a finite normal reflection.<sup>30</sup> Note that also for finite, but

relatively large transparency,  $Z \sim 1$ , there are the same two  $0 - \pi$  transitions as in fully transparent junctions, although the critical current exhibits rapid oscillations due to the resonant amplification. The same result holds for the corresponding planar junctions after summation over transverse channels, even for a small transparency of interfaces.<sup>12</sup>

Temperature-induced transitions both from  $0$  to  $\pi$  and from  $\pi$  to  $0$  are studied by computing the phase diagram with temperature and junction width as variables, for different interfacial transparencies from metallic to tunnel limit, Fig. 7. In the case of low transparency there is a  $0 - \pi$  transition for each  $d$  where the quasibound states cross the Fermi surface. The characteristic non-monotonic dependence of  $I_C(T)$  with a well-pronounced dip at the transition is shown in Figs. 8 and 9, with the corresponding parts of the phase diagram in the insets. One can see that the  $\pi$  state can correspond to lower temperatures than the  $0$  state. In Figs. 10 and 11 Andreev levels and their contributions to  $I(\phi)$  are shown for three temperatures. Note that the discussed mechanism of  $0 - \pi$  transition is more general and robust against the insertion of scattering centers into the F interlayer. Similar results are previously obtained for a diffusive point contact connecting two SF bilayers (SFcFS).<sup>2</sup>

### III. CONCLUSION

We have shown the resonant nature of  $0 - \pi$  transitions in short ballistic SIFIS junctions with one transverse channel open for propagation. Unlike the corresponding SINIS structures, in low-transparency SIFIS junctions the peaks in  $I_C(d)$  curves do not reach the corresponding value for transparent junctions; instead, the  $0 - \pi$  transitions are triggered and narrow dips open up exactly at the peaks. This is not the case for higher interface transparency, nor for planar junctions.

We have shown that the rule: "The  $\pi$  state is characterized by net spin polarization of the current-carrying Andreev levels"<sup>26,28</sup> is not quite general. Remaining true for high-transparency junctions, in SIFIS tunnel junctions the situation can be the opposite. We generalized the previous rule to read as follows:  $0 - \pi$  transition is accompanied by the switching of net spin polarization of current-carrying Andreev levels. In agreement with experimental observations,<sup>6</sup> we also demonstrated that in the phase diagram of double-barrier SIFIS junctions the  $\pi$  state can occur at lower temperatures than the  $0$  state (or the other way round), depending on parameters. This also holds for planar double-barrier junctions,<sup>12</sup> as well as for diffusive SFcFS point contacts.<sup>2</sup>

## ACKNOWLEDGMENTS

This work has been supported by the Serbian Ministry of Science, Project No. 141014, and by Franco-Serbian PAI EGIDE Project No. 11049XG. NMC also acknowledges the support of RFBR Project No. 03-02-16677,

No. 04-02-08159, and No. 06-02-17519, the Russian Ministry of Science, the Netherlands Organization for Scientific Research NWO, CRDF, and Russian Science Support Foundation.

- 
- <sup>1</sup> A. I. Buzdin, *Rev. Mod. Phys.* **77**, 935 (2005).  
<sup>2</sup> A. A. Golubov, M. Yu. Kupriyanov, and E. Il'ichev, *Rev. Mod. Phys.* **76**, 411 (2004).  
<sup>3</sup> L. N. Bulaevskii, V. V. Kuzii, and A. A. Sobyanin, *Pis'ma Zh. Eksp. Teor. Fiz.* **25**, 314 (1977) [*JETP Lett.* **25**, 290 (1977)].  
<sup>4</sup> A. I. Buzdin, L. N. Bulaevskii, and S. V. Paniukov, *Pis'ma Zh. Eksp. Teor. Fiz.* **35**, 147 (1982) [*JETP Lett.* **35**, 178 (1982)].  
<sup>5</sup> Z. Radović, M. Ledvij, L. Dobrosavljević-Grujić, A. I. Buzdin, and J. R. Clem, *Phys. Rev. B* **44**, 759 (1991).  
<sup>6</sup> V. V. Ryazanov, V. A. Oboznov, A. Yu. Rusanov, A. V. Veretennikov, A. A. Golubov, and J. Aarts, *Phys. Rev. Lett.* **86**, 2427 (2001).  
<sup>7</sup> T. Kontos, M. Aprili, J. Lesueur, and X. Grison, *Phys. Rev. Lett.* **86**, 304 (2001).  
<sup>8</sup> A. Bauer, J. Bentner, M. Aprili, M. L. Della-Rocca, M. Reinwald, W. Wegscheider, and C. Strunk, *Phys. Rev. Lett.* **92**, 217001 (2004).  
<sup>9</sup> J. S. Jiang, D. Davidović, D. H. Reich, and C. L. Chien, *Phys. Rev. Lett.* **74**, 314 (1995).  
<sup>10</sup> Y. Obi, M. Ikebe, and H. Fujishiro, *Phys. Rev. Lett.* **94**, 057008 (2005).  
<sup>11</sup> T. Yamashita, K. Tanikawa, S. Takahashi, and S. Maekawa, *Phys. Rev. Lett.* **95**, 097001 (2005).  
<sup>12</sup> Z. Radović, N. Lazarides, and N. Flytzanis, *Phys. Rev. B* **68**, 014501 (2003).  
<sup>13</sup> J. Cayssol, and G. Montambaux, *Phys. Rev. B* **70**, 224520 (2004).  
<sup>14</sup> K. Halterman and O. T. Valls, *Phys. Rev. B* **70**, 104516 (2004); **69**, 014517 (2004).  
<sup>15</sup> D. Bohm, *Quantum Theory* (Prentice-Hall, New York, 1951).  
<sup>16</sup> C. W. J. Beenakker, *Phys. Rev. Lett.* **67**, 3836 (1991).  
<sup>17</sup> C. W. J. Beenakker and H. van Houten, *Phys. Rev. Lett.* **66**, 3056 (1991).  
<sup>18</sup> J. A. Melsen and C. W. J. Beenakker, *Physica B* **203**, 219 (1994).  
<sup>19</sup> S. E. Shafranjuk and J. B. Ketterson, *Phys. Rev. B* **72**, 024509 (2005).  
<sup>20</sup> Z. Radović, L. Dobrosavljević-Grujić, and B. Vujičić, *Phys. Rev. B* **63**, 214512 (2001).  
<sup>21</sup> H. Sellier, C. Baraduc, F. Lefloch, and R. Calemczuk, *Phys. Rev. Lett.* **92**, 257005 (2004).  
<sup>22</sup> H. Takayanagi, T. Akazaki, and J. Nitta, *Phys. Rev. Lett.* **75**, 3533 (1995).  
<sup>23</sup> S. Gueron, Mandar M. Deshmukh, E. B. Myers, and D. C. Ralph, *Phys. Rev. Lett.* **83**, 4148 (1999).  
<sup>24</sup> E. Scheer, N. Agrait, J. C. Cuevas, A. L. Yeyati, B. Ludoph, A. Martin-Rodero, G. R. Bollinger, J. M. van Ruitenbeek, and C. Urbina, *Nature* **394**, 154 (1998).  
<sup>25</sup> S. K. Yip, *Phys. Rev. B* **62**, R6127 (2000).  
<sup>26</sup> Y. Tanaka and S. Kashiwaya, *Physica C* **274**, 357 (1997).  
<sup>27</sup> N. M. Chtchelkatchev, W. Belzig, Yu. V. Nazarov, and C. Bruder, *Pis'ma Zh. Eksp. Teor. Fiz.* **74**, 357 (2001) [*JETP Lett.* **74**, 323 (2001)].  
<sup>28</sup> Yu. S. Barash and I. V. Bobkova, *Phys. Rev. B* **65**, 144502 (2002).  
<sup>29</sup> N. M. Chtchelkatchev, *Pis'ma Zh. Eksp. Teor. Fiz.* **80**, 875 (2004) [*JETP Lett.* **80**, 12 (2004)].  
<sup>30</sup> M. Božović and Z. Radović, *Phys. Rev. B* **66**, 134524 (2002).
- Fig. 1 A schematic of a double-barrier superconductor-ferromagnet-superconductor junction.  $I_1$  and  $I_2$  denote the insulating layers.
- Fig. 2 Critical Josephson current  $I_C$  as a function of the normal-metal-interlayer thickness  $d$  at zero temperature for transparent ( $Z = 0$ , dotted curves) and low-transparency ( $Z = 10$ , solid curves) interfaces, for the SINIS junction ( $X = 0$ , top panel) and the SIFIS junction ( $X = 0.1$ , bottom panel). Note that  $I_C(d)$  for low-transparency SIFIS junction is magnified 20 times.
- Fig. 3 A peak in  $I_C(d)$  and the spin degenerate Andreev levels,  $E(\phi_C)$ , for a SINIS junction with  $Z = 10$  and  $X = 0$  at zero temperature.
- Fig. 4 Two neighboring peaks in  $I_C(d)$  for the SIFIS junction with  $X = 0.1$  and  $Z = 10$ , and spin split Andreev levels,  $E(\phi_C)$ : two spin up levels (thick and thin solid curves) and two spin down levels (thick and thin dashed curves). Insets: dips at  $0 \leftrightarrow \pi$  transitions.
- Fig. 5 Variation of the Andreev levels as a function of the phase difference  $\phi$  for five values of the normal-layer thickness indicated in the inset of Fig. 4, with all other parameters being the same. The arrows indicate the spin polarization of the levels.
- Fig. 6 The current-phase relation (solid curves) for five values of the normal-layer thickness indicated in the inset of Fig. 4, with all other parameters being the same. Partial currents carried by the corresponding Andreev levels shown in Fig. 5 are also presented (dotted curves).
- Fig. 7 The phase diagram as a function of the normalized temperature  $T/T_C$  and normalized ferromagnetic-layer thickness  $dk_F$ , for transparent ( $Z = 0$ , top panel) and low-transparency interfaces ( $Z = 10$ , bottom panel), and for  $X = 0.1$ .
- Fig. 8 Characteristic temperature variation of  $I_C$  showing the temperature-induced transition from 0 to  $\pi$  states for a junction width  $dk_F = 32.755$ ,  $X = 0.1$ , and  $Z = 10$ . The inset shows the part of the phase diagram for the corresponding transition.

Fig. 9 Characteristic temperature variation of  $I_C$  showing the temperature-induced transition from  $\pi$  to 0 states, for a junction width  $dk_F = 59.708$ ,  $X = 0.1$ , and  $Z = 10$ . The inset shows the parts of the phase diagram for the corresponding transition.

Fig. 10 Variation of the Andreev levels as a function of the phase difference  $\phi$  for  $dk_F = 29.609$ ,  $X = 0.1$ , and  $Z = 10$ . The arrows indicate the spin polarization of the levels.

Fig. 11 The current-phase relation (solid curves) for the same parameters as in the Fig. 10, and for three different temperatures: (1)  $T/T_C = 0.01$ , (2)  $T/T_C = 0.2$ , and (3)  $T/T_C = 0.5$ . Partial currents carried by the corresponding Andreev levels are also presented (dotted curves).

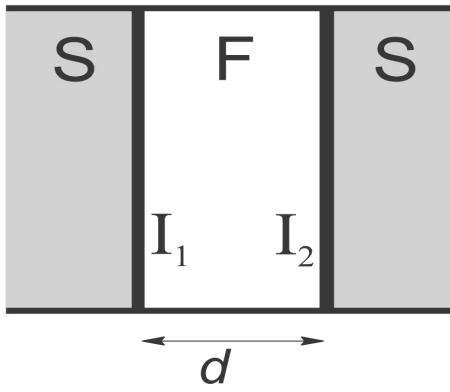


FIG. 1:

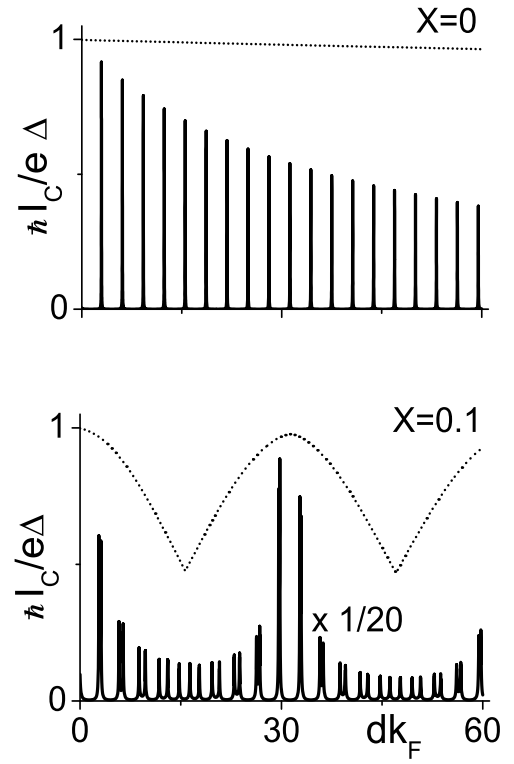


FIG. 2:

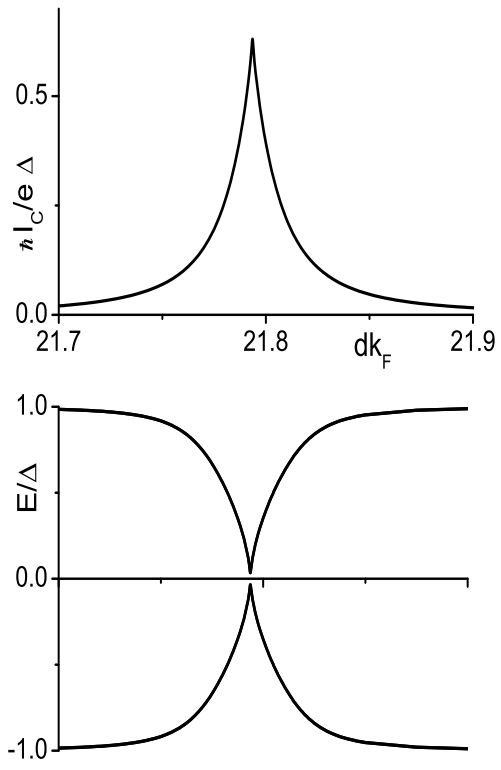


FIG. 3:

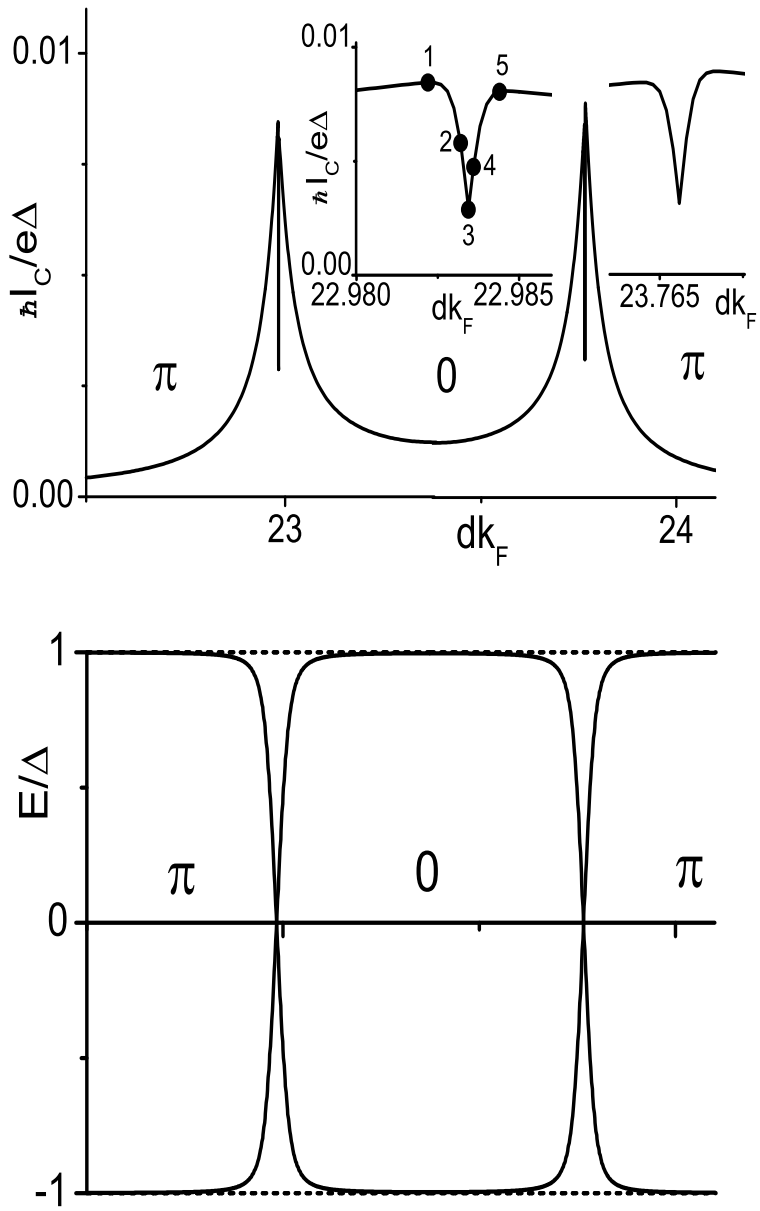


FIG. 4:

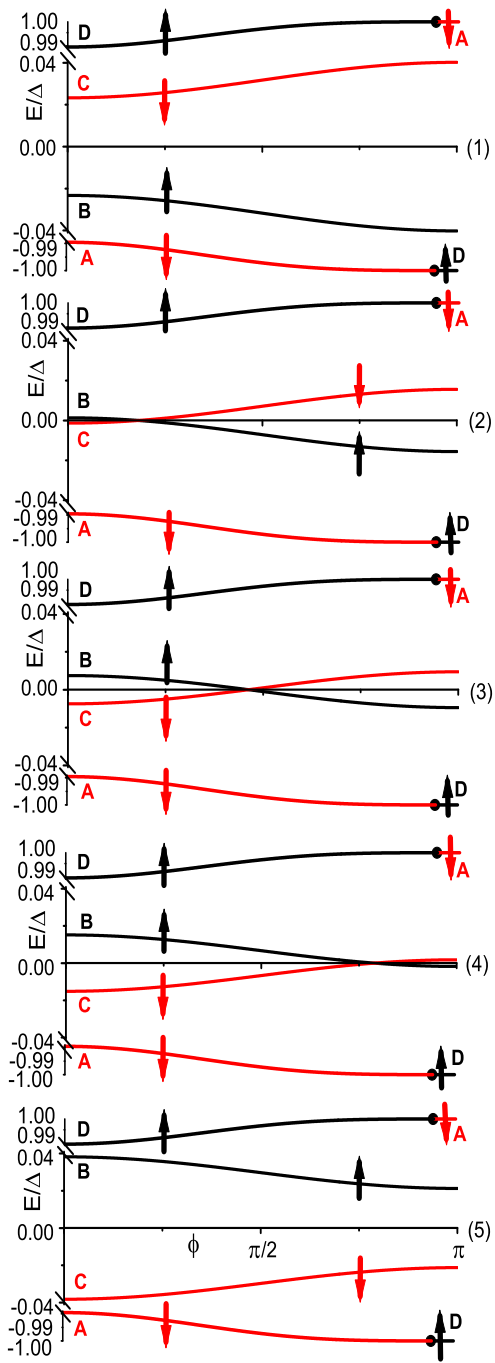


FIG. 5:

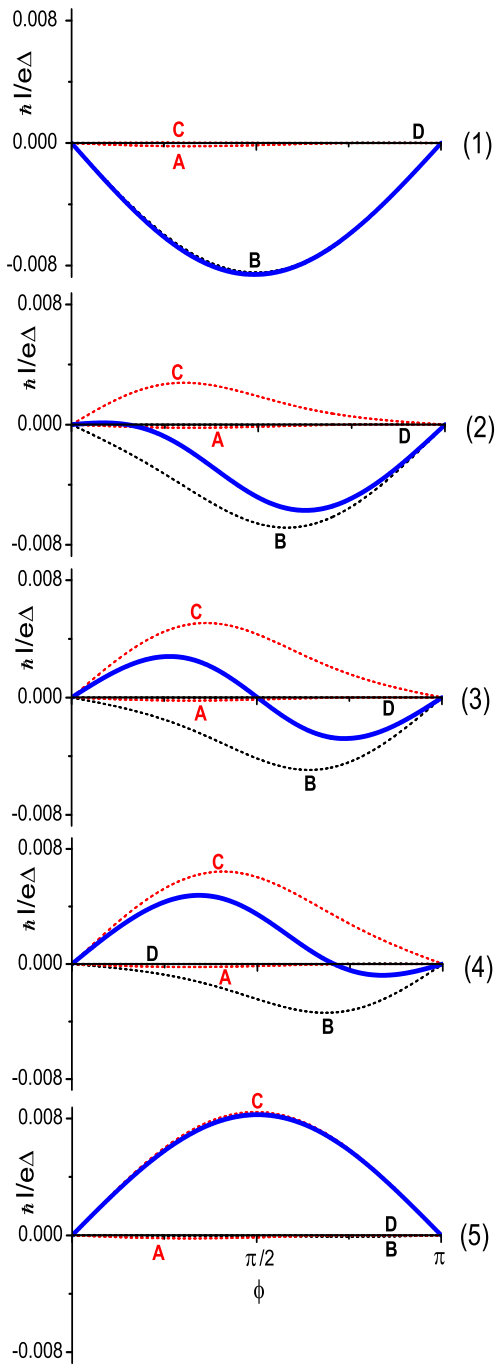


FIG. 6:

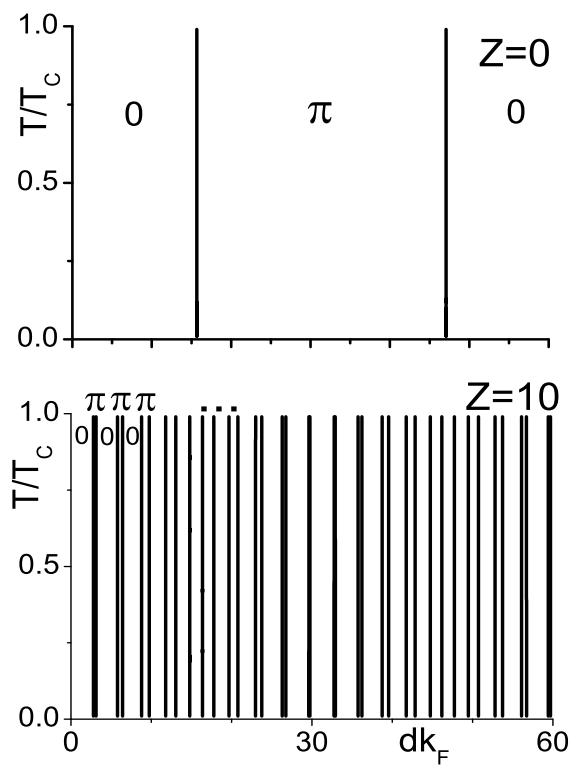


FIG. 7:

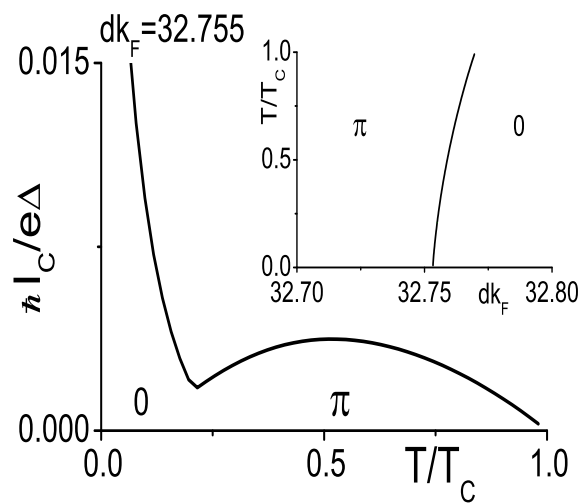


FIG. 8:

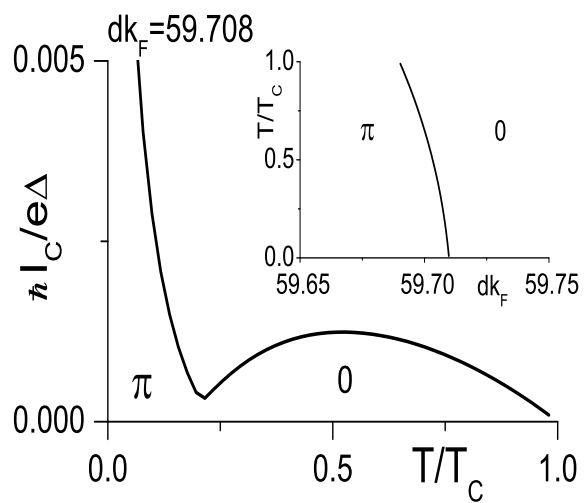


FIG. 9:

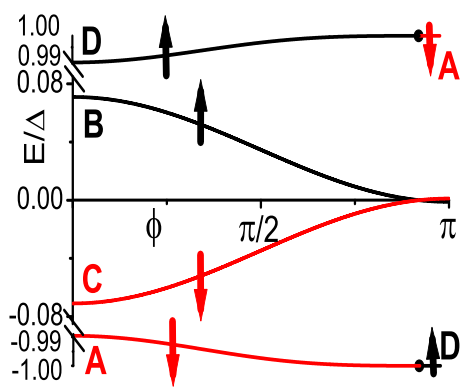


FIG. 10:

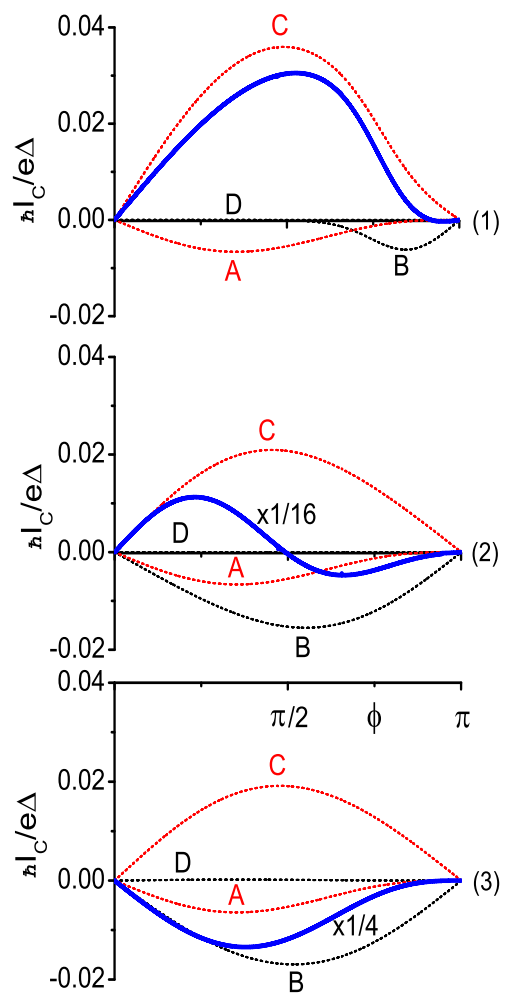


FIG. 11: